Continuous Blood Pressure Monitoring Using Nonpulsatile Photoplethysmographic Components for Low-Frequency Vascular Unloading

Tuukka Panula, Jukka-Pekka Sirkiä, and Matti Kaisti

***Abstract*— Continuous blood pressure (BP) monitoring gives a better understanding of a person's cardiovascular health status than single BP measurements. The existing measurement techniques are often highly complex and expensive or suffer from inaccuracies. We propose a simple, yet effective technique for continuous BP monitoring. Our method is based on the finding that the nonpulsatile (dc) component of the photoplethysmograph (PPG) correlates with BP. By keeping the infrared (IR) PPG dc component constant by altering the applied external pressure using a feedback mechanism, the BP can be measured continuously. This way the pressure reading from the pressure sensor follows the mean intraarterial BP. We call this low-frequency vascular unloading. We propose a method for assessing the measurement error introduced by changes in vasomotor tone. Green PPG was used for the vasomotor compensation method. We packaged the technology into a wearable finger-worn device similar to a pulse oximeter probe. We measured over 90 min of continuous BP data from a total of seven subjects. The subjects were asked to perform different BP-altering maneuvers during the measurement. The ability to track BP changes was verified by continuous mean arterial pressure (MAP) readings measured with the reference device (CNSystems CNAP 500) and our device, resulting in the correlation of $r = 0.894$ and [(mean ± SD) mmHg] of (0.3 ± 4.3) mmHg for MAP. Without vasomotor tone compensation (VMC), the results were slightly less accurate: $r = 0.83$, (−1.4 ± 5.1) mmHg. The proposed technology performed well compared to the traditional vascular unloading technique (VUT) while requiring significantly less complex control logic and no fast-switching pneumatics. The proposed technique is a simple, yet effective, low-cost solution and it can be constructed from off-the-shelf components and miniaturized into a wearable form factor. The technique has potential in the field of health wearables and remote continuous BP monitoring for personalized health applications.**

***Index Terms*— Biomedical monitoring, hypertension, medical instruments, photoplethysmography, pressure sensors.**

Manuscript received 8 December 2022; revised 6 March 2023; accepted 19 March 2023. Date of publication 14 April 2023; date of current version 5 May 2023. This work was supported in part by Business Finland under Project 1574/31/2018. The work of Tuukka Panula was supported in part by the Emil Aaltonen Foundation and in part by the Finnish Foundation for Technology Promotion. The Associate Editor coordinating the review process was Dr. Jae-Ho Han. *(Corresponding author: Tuukka Panula.)*

This work involved human subjects or animals in its research. Approval of all ethical and experimental procedures and protocols was granted by the Ethical Committee of the Hospital District of Southwest Finland and the National Supervisory Authority for Welfare and Health, and performed in line with the Declaration of Helsinki.

The authors are with the Department of Computing, University of Turku, 20500 Turku, Finland (e-mail: tuukka.j.panula@utu.fi; jpsirk@utu.fi; mkaist@utu.fi).

Digital Object Identifier 10.1109/TIM.2023.3267378

I. Introduction

MEASURING blood pressure (BP) continuously and noninvasively is a significant challenge with academic and industrial interests alike. Instead of a single measurement, it is acknowledged that multiple subsequent measurements taken over a longer time period give a better understanding of a person's health status [1]. Diagnosing hypertension reliably requires data to be collected for preferably 24 h [2]. This is most often achieved by wearing an ambulatory cuff-based BP monitor throughout the day and measuring, for example, every 30 min. Nocturnal or night-time BP tracing is considered to be an accurate diagnostic tool for assessing hypertension [3]. Based on nocturnal BP tracing, patients are categorized into dippers and nondippers by a surge in BP or absence of it. Even with an automated ambulatory cuff device, important phenomena can be missed. Moreover, traditional brachial cuff-based devices are bulky and inconvenient to use, easily interrupting one's sleep. Several methods have been introduced to tackle these challenges. Additionally, they could provide an alternative to arterial catheterization in invasive medical procedures. Recent developments, in the field of BP instrumentation, show a trend toward wearables and continuous BP monitoring [4].

The vascular unloading technique (VUT) or volume clamp method was invented by the Czech physiologist Jan Peňáz in 1973 [5]. A VUT device uses a feedback control loop system that applies counter pressure to a finger cuff to keep the optical blood flow signal constant during each cardiac cycle. The pressure measured from the cuff then equals intraarterial pressure. The system relies on a set of pumps and valves used at a high switching frequency to control the pressure. This technique has been proven in multiple studies over the decades.

Other cuffless methods for measuring continuous BP have been proposed, including tonometry [6], [7], pulse propagation [8], [9], [10], [11], and pulse waveform analysis [12], [13], [14], [15]. However, all these methods require individual calibration and their accuracy has been questioned [4], [16].

A photoplethysmograph (PPG) signal consists of two components: alternating current (ac) and direct current (dc) components [18]. The former corresponds to the pulsatile blood flow in the artery and the latter is considered the nonpulsatile composite of the steady venous and arterial blood volume in the underlying tissue. A study comparing intraarterial BP to

a PPG signal showed a clear correlation between BP and the PPG dc components [18]. In 2021, we proposed a conference article introducing a control method that uses the infrared (IR) dc component as a reference to control external contact pressure to minimize transmural pressure (P_t), that is, the difference between arterial pressure and externally applied pressure, enabling continuous BP measurement [19]. Here, we further refine this method and provide more measurements. We also introduce a method for assessing the measurement error introduced by changes in vasomotor tone with green PPG dc components. VUT devices typically use some form of setpoint correction to compensate for vasomotor changes. The literature recognizes three methods for readjusting the setpoint during the measurement [20]. Finapres uses "Physiocal," where they open the feedback loop for a few seconds and assess the pulse volume at positive and negative P_t [21]. Based on the pulse volume, the setpoint is adjusted. CNAP uses a very similar approach called "VERIFI," where they compare the optical pulse shape to the original one acquired at the calibration stage [22]. This method has the advantage of not having to pause the measurement during setpoint assessment. The last method, dynamic vascular compliance (DVC), uses superimposed pressure vibrations to see whether the P_t has changed [20]. We studied whether changing vasomotor tone could be estimated using postprocessing techniques without affecting the measurement itself. We built a pulse oximeter form factor finger device consisting of the sensors and actuators needed for implementing the proposed technique.

We believe that the use of green PPG in measuring changes in arteriolar volume could be used to assess changes in vasomotor tone and thus improve the accuracy of BP measurements. For example, when a significant drift in vasomotor tone is detected, the device could initiate an oscillometric recalibration. Additionally, it could be used to verify the integrity of the measurement afterward. We noticed that the green dc-level does change during actual BP changes as well as IR PPG. However, it is expected that vasomotor action (including Meyer waves at <0.1 Hz) happens at a considerably lower rate than the induced pressure changes and thus it can be used for compensation independent of the IR PPG dc [23]. The vasomotor tone compensation (VMC) that can be applied postmeasurement could prove useful in, for example, nocturnal BP monitoring, where the analysis is done after the full measurement. Since postprocessing is not applicable during real-time BP tracing, a method for reassessing the setpoint during the measurement should be added to the presented method for improved tracking capability. Using the green dc-level added to the IR signal could provide a way to track both BP changes and vasomotor changes. Instead of only the IR dc-level, a composite of IR and green dc-levels could be used for volume clamping.

CNSystems introduced a modified volume clamp method (CNAP2GO) that does not clamp the full cardiac cycle [24]. Instead, it computes the area under each pulse and this way readjusts the counter pressure to make sure the pulse waveform stays unchanged. The adjustment is done once for every cardiac cycle. The method was implemented on a modified CNAP 500 device, but the research group also demonstrated a way to miniaturize the technique.

While the volume clamp method is a powerful tool, it has some limitations. Because it is based on clamping the full cardiac cycle, the technique requires very fast-switching pneumatics. These systems are not easy to miniaturize and usually require a separate finger probe and a costly main unit. The CNAP2GO, while still using a cuff, manages to overcome this by applying much lower frequency volume clamping. CNAP2GO was implemented on a CNAP 500 device with modified firmware. In addition, the authors proposed a battery-operated miniaturized version. We believe that our approach is cost-efficient compared to the previous methods, since it uses low-cost off-the-shelf components. Additionally, since it does not require a cuff, the technology can be integrated into a pulse oximeter form factor, as shown in Fig. 1.

Commercial smartwatch-based devices have been introduced to provide a wearable method to measure BP. Such devices include the Heartguide (Omron, Japan), which uses wrist cuff oscillometry and BPro G2 (Bpro, Ireland), which uses applanation tonometry. Heartguide can be programed to take spot BP measurements at predefined intervals but is not capable of acquiring BP continuously. BPro G2 can obtain up to 24 h of continuous BP, but requires an initial calibration and setup done at the physician's office [6], [25].

This article is structured as follows: we first describe the sensors, mechanics, and software used for implementing the proposed technique. Then we explain the three phases of operation—open-loop action, closed-loop action, and postprocessing—which are used to obtain the final continuous BP tracing. Next, we present the results from the actual human studies before conclusions.

II. Methods

A. System Operation

The device operation can be divided into three segments: open-loop action, closed-loop action, and postprocessing. This is summarized in Fig. 2.

1) Open-Loop Action: Similar to VUT, the proposed technique relies on an initial calibration used to find the initial setpoint, for example, the level of zero P_t [20]. At this point, the transfer of the pulsatile signal to the sensor is at its maximum. Finding the setpoint is done using open-loop control. An increasing pressure ramp is introduced to the finger and the pressure ramp is stopped when reaching a predefined suprasystolic value (140 mmHg in most cases). Using bandpass filtering and Hilbert transform, the point of maximum pulsation in the pressure curve is found. This marks the level of finger mean arterial pressure ($\text{MAP}_{\text{finger}}$) and zero P_t. The external pressure is then set to this level and the desired setpoint is calculated by computing the mean dc level from five subsequent IR PPG pulses. At the beginning of a measurement, a brachial cuff measurement is taken and the pressure signal is calibrated to the brachial MAP provided by the reference device. It must be noted that due to pulse reflection and amplification, the brachial and finger pressures

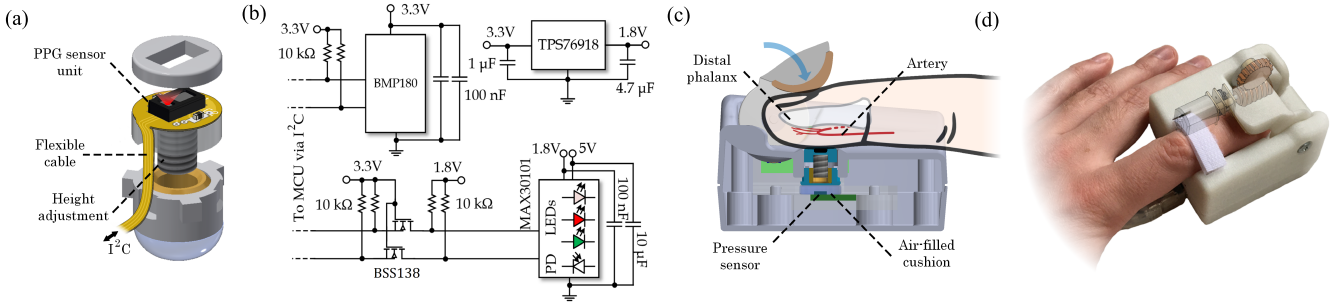

Fig. 1. Device structure. (a) Sensor piston is composed of a top part housing the PPG electronics and a bottom part with an air cushion. The parts are connected by a threaded shaft, enabling height adjustment. (b) Sensor schematics. The PPG module (MAX30101) is housed on a custom PCB along with level-shifting MOSFETs (BSS138) and a voltage regulator (TPS76918). ON-board voltage shifting and regulation is needed since the LEDs require a 5-V supply, the PPG module itself uses 1.8-V logic and the MCU operates at 3.3 V. The PPG module has a transparent window for the LEDs and the photodiode. The module is in direct contact with the skin. The pressure sensor (BMP180) is located on a separate PCB. (c) Piston transfers the arterial pulsation from the finger to the pressure sensor fixed to the housing. (d) Photograph of the device in use. The press is manipulated by a dc motor via a set of gears. A Velcro strap is used to fix the finger in place firmly. The mechanics are described in more detail elsewhere [17].

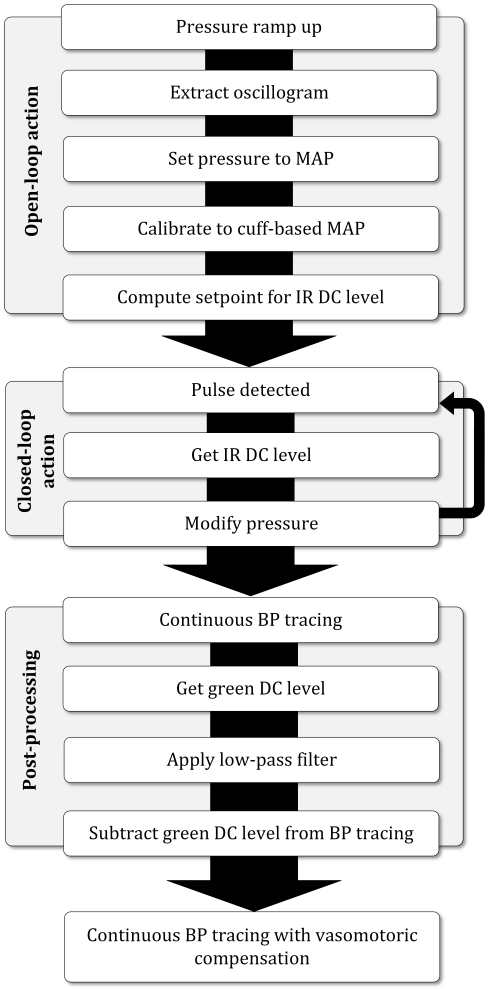

Fig. 2. Block diagram illustrating the device operation. Open-loop computation and post-processing are done at the PC end, and closed-loop action is fully executed in the MCU.

differ slightly. Although this has a greater effect on SBP and DBP, some effect is apparent on MAP as well. In this study, we believe that we can minimize this effect by calibrating both devices to the same brachial MAP value outputted by the reference device CNAP 500.

2) Closed-Loop Action: After the initial calibration phase, the system proceeds to the actual BP tracking phase, which uses a closed-loop feedback system. The system is "closed" since it uses a feedback signal to adjust its input. Traditional VUT systems control the volume between and during each cardiac cycle. This means that the IR PPG volume is kept constant during the periodic changes, within and across cardiac cycles, caused by pulsatile blood flow. The controller can sample the volume hundreds of times during each pulse. Instead of "clamping" the full cardiac cycle, in our method, only the average volume over a cardiac cycle is controlled and kept at a constant level. This is accomplished by taking the mean value of each cardiac cycle and making only one volume compensating maneuver once in a cardiac cycle. This low-frequency vascular unloading is much less computationally intensive than traditional VUT. After detecting a pulse, the system computes the dc value individually for the pulse by integrating it over one cardiac cycle. The dc level is passed to the controller only after each pulse and the controller refresh rate is much slower, actually the same as the heart rate, and not dependent on the sensor sampling frequency. A PID controller is used to keep the dc-level of the IR PPG signal constant by modifying the counter pressure directed to the finger. This allows the pressure sensed at the piston to follow mean intraarterial pressure. In our case, the IR level oscillates a bit around the setpoint, but since BP is computed as an average of multiple pulses, it has minimal effect on the results. Operation of the feedback system is shown in Fig. 3(a).

3) Postprocessing: Our device does not implement any real-time setpoint correcting methods which can introduce an error in the measurement due to changes in vasomotor tone. We aimed to solve this by creating a method for recognizing and compensating for these changes in vasomotor tone. This VMC is done postmeasurement and no interruptions to the measurement are required. IR and red wavelengths in PPG are known to probe the volume of the larger subcutaneous arteries [26]. Similarly, green PPG is known to only penetrate the dermis, which populates smaller arterioles [26]. Arterioles are the conducting vessels between arteries and capillaries and are responsible for the majority of vasomotor tone [23]. When clamping the arterial volume via IR PPG, the arteriolar volume is allowed to vary freely. This is seen in the green PPG dc-component, where vasodilation exhibits an upward

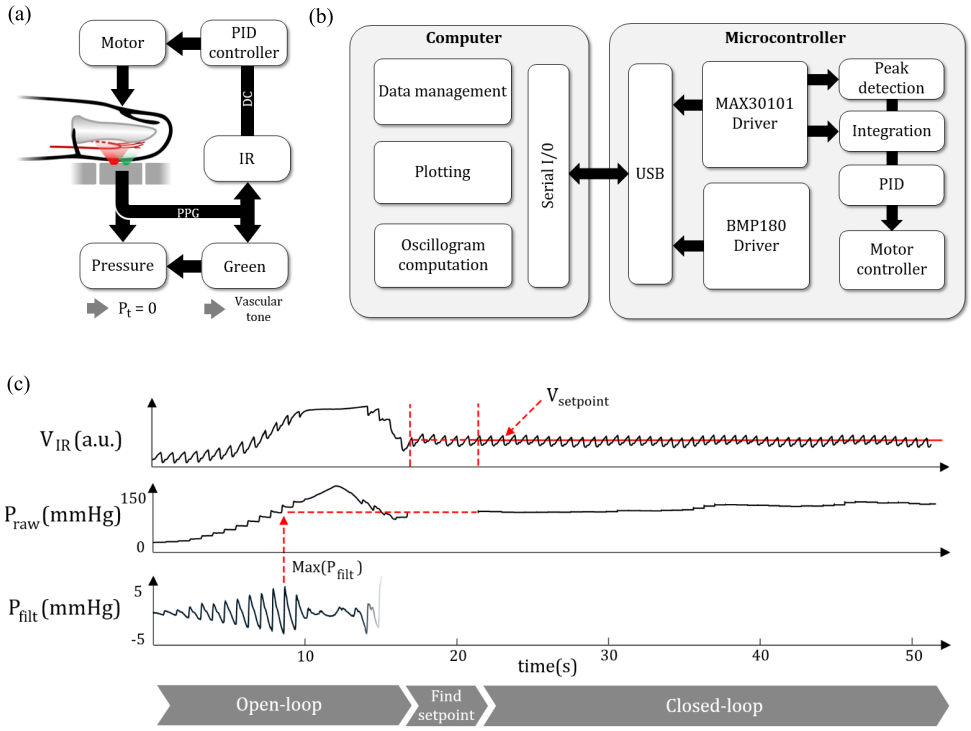

Fig. 3. System operation. (a) Motorized press is used to apply pressure to the finger. The dc component acquired from the unfiltered IR PPG signal is used to control the applied pressure applied. The control logic ensures that transmural pressure (P_t) is kept at near zero mmHg and the pressure reading from the pressure sensor equals MAP. Green wavelength is used for assessing the vascular tone. (b) Block diagram showing software/firmware functionality. Interfacing is done via USB. (c) Proposed method for clamping beat-wise arterial volume. The procedure begins with the open-loop action, where contact pressure is swept to suprasystolic pressure and the point of maximum pulsation Max(P_{filt}) is found. Next, the contact pressure is lowered to the corresponding pressure and held there for the duration of five IR PPG pulses. These pulses are averaged, resulting in V_{setpoint}, which is the setpoint volume used for volume clamping. The final phase is the closed-loop action, where the PID controller is used to keep IR PPG dc-level at V_{setpoint}. When this is true, the pressure sensed at the pressure sensor P_{raw} equals intraarterial pressure. In the close-loop section, the device only outputs a mean value for each pulse.

shift in the dc-level and vice versa for vasoconstriction. We demonstrated the green PPG's ability to track vasomotor action by summing the green dc-component multiplied by a constant k and the raw pressure signal P. k was the same in each measurement found empirically. It is likely that on a different type of system or sensor, the value has to be defined separately. V_G represents the blood volume measured by green PPG. The dc-component V_{G_lowpass} is extracted by applying a lowpass filter to V_G. The resulting signal P_{VMC} is the pressure with vasomotor tone compensated

$$P_{\text{VMC}} = P + kV_{G\_\text{lowpass}}.$$

B. Sensor Structure

Instead of an inflatable cuff, the technology is based on motor-actuated finger pressing and a tonometric sensor setup. The sensor system comprises a piston, a PPG module MAX30101 (Maxim Integrated, USA), and a barometric pressure sensor BMP180 (Bosch Sensortec, Germany). The wavelengths for the integrated LEDs in the module are 880 and 537 nm for IR and green, respectively. The PPG module is soldered on a flexible polyimide printed circuit board (PCB) with a thickness of 0.1 mm and then placed on top of the piston. The most vulnerable point is the 90° angle between the sensor and the side of the piston. However, the piston is constructed so that the bend radius here is roughly 1 mm and the setup is performed without any complications. The module is connected to the power supply and MCU via a flexible flat cable. The cable is run parallel to the piston and connected to a PCB populating interface electronics. These include level-shifting MOSFETs (BSS138, Onsemi, USA) and a low dropout voltage regulator (TPS76918, Texas Instruments, USA). ON-board voltage shifting and regulation is needed since the LEDs require a 5-V supply, the PPG module itself uses 1.8-V logic and the MCU operates at 3.3 V. The PPG module has a transparent window for the LEDs and the photodiode. The module is in direct contact with the skin. The opposite end of the piston has an air cushion attached to it. Fig. 1(a) shows the piston construction. The piston is used to apply pressure to a barometric pressure sensor through the air cushion. The pressure sensor is housed on a separate PCB. This way, the pressure applied to the piston is directed to the piezoelectric sensing element. The principle is shown in Fig. 1(b). The piston has a threaded shaft separating the top and bottom halves, allowing its height to be modified during assembly. The piston parts are manufactured using 3-D printing.

The technology is packaged into a wearable finger-worn device similar to a pulse oximeter probe. A small dc motor (generic N20 brushed dc motor) is used to apply pressure to

the finger via a set of gears and a hinged press. The press is lined with soft 3-D printed plastic to avoid discomfort during the measurement. A complete system description including the mechanical and electrical design is described in our previous conference article [17]. The finished instrument with the inner power train visible is seen in Fig. 1(c). Fig. 3(a) shows the system structure.

C. Software

1) PC Software: Interaction with a PC is done via a graphical user interface (GUI) written in Python. The application connects to the device through a USB serial connection, which is used to send commands and receive data. The application plots the incoming data in real time. Open-loop action is controlled by the Python application. The oscillogram and the pressure where max oscillations occur are computed at the PC end. These maximum oscillations correspond to the MAP, which is also the point of zero P_t. We find this pressure level with the following steps: Oscillometric waveform envelope (OMWE) is obtained by: 1) first applying a Butterworth bandpass filter (1–10 Hz) to the pressure ramp signal and then applying; 2) Hilbert transform; 3) by finding the peaks of the resulting signal; and 4) by fitting a polynomial curve through them, we can acquire the envelope [27]. The maximum point of the envelope is used to find the zero P_t level on the corresponding pressure ramp.

The application gives the device firmware the initial pressure value and a command to start closed-loop action. From this point on, the device operates independently, only sending measurement values to the application. The GUI also has a dedicated button for initiating an open-loop calibration at any time during the continuous BP measurement.

2) Firmware: We chose nRF52 (Nordic Semiconductor, Norway) family system-on-chip (SoC) as the microcontroller unit (MCU) due to its processing power and interface capabilities. The MCU (nRF52840) houses ARM's Cortex M4 processing core. Device firmware was written in C. Proportional-integral-derivative (PID) controller and mathematic operations were implemented with ARM Common Microcontroller Software Interface Standard (CMSIS) library using 32-bit floating-point arithmetics. The PID controller was at first rough-tuned using the Ziegler–Nichols method [28]. This was followed by further fine-tuning for optimized performance of the feedback control. Both the pressure sensor and the PPG sensor are sampled at 100 Hz.

The MCU firmware is solely responsible for closed-loop action and apart from the initial pressure value, does not rely on external processing at the PC end. Real-time peak detection, pulse mean value calculation, and control logic are done ON-board. Sampled at 100 Hz, the last 45 IR data samples are continuously divided into three 15-sample segments and averaged. A pulse foot is considered to be found if the middle segment has a value larger than both outer segments. The trapezoidal integral is then calculated over the single pulse to find its mean-or dc-level. This value is then passed to the PID controller. The controller takes the dc level as input and outputs a value ranging from −50% to 50%. This value represents the duty cycle and direction for the motor driver. Immediately after detecting a pulse, the motor is driven for 30 ms as dictated by the PID controller. If no pulse is detected for a period of 3 s, the system assumes the counter pressure is too high and releases pressure until the pulse appears again. The real-time signal processing methods applied at the MCU end are simple but performed well under the test conditions. However, more advanced and robust methods could be implemented for better reliability in adverse measurement conditions. Interaction of the PC software and embedded firmware is shown in Fig. 3(b).

3) Signal and Statistical Analysis: Signal postprocessing and statistical analysis were done on MATLAB R2019a. For extracting the green dc level, we applied a sixth-order Butterworth low-pass filter with a cutoff frequency of 0.025 Hz. This dc level (V_{G_lowpass}) was used for VMC.

Statistical analysis includes computing correlation and Bland–Altman plots. BP measurement points were sampled at 10 s segments with 5 s overlap for both the developed device and reference device. This results in a total of 563 paired BP samples for comparison. Both devices were sampled at 100 Hz. Synchronizing the signals was achieved by stopping both devices at the same time. The reference device outputs the raw pressure data file as well as a file containing averaged SBP, DBP, and MAP readings.

D. Human Studies

We took repeated measurements from seven subjects (age: 26–77, three females) resulting in a total of 90 min of BP data with dynamic changes. Two of the subjects were on BP medication. The average length for measurement was 8 min excluding open-loop action. The reference device is a state-of-the-art VUT device (CNSystems CNAP 500) [29]. We had a repertoire of BP-altering maneuvers (fast breathing, deep breathing, and passive leg raising) to be used to induce a visible change in BP. Not all subjects showed a significant response to every maneuver, so we selected the ones with the largest response. The responsivity was tested before taking the actual measurement. Measurements were made with CNAP 500 worn on the middle and ring fingers and our device on the index finger ipsilaterally with the subject in a supine position. Initial BP was taken using the integrated brachial cuff in the reference device. Both devices were calibrated using the same reference value. The measurements were conducted according to the Declaration of Helsinki guidelines with the permission of the Ethical Committee of the Hospital District of Southwest Finland and the National Supervisory Authority for Welfare and Health [30].

III. Results

A. Impact of Closed-Loop Control

We took measurements with the closed-loop feedback switched off and observed how BP-altering maneuvers would affect the signals. In Fig. 4(a), we see the pressure steadily decreasing along with the IR dc component. At approximately 160 s, the subject performed deep breathing resulting in a sudden drop in the BP. Here, the IR level actually increases, suggesting that the applied pressure is now higher than MAP. This is also indicated by the diminishing IR pulse pressure. In this case, if the feedback were on, the controller would

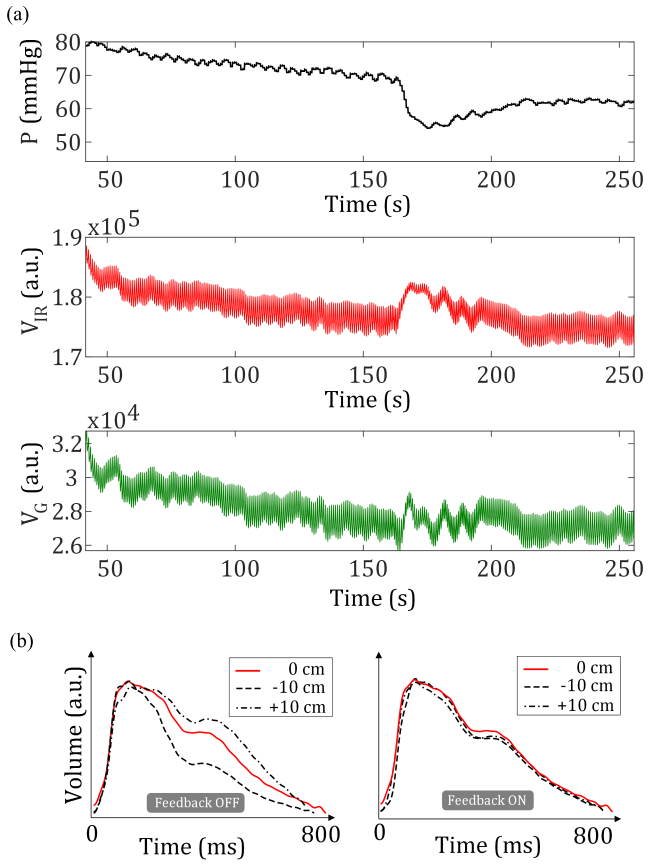

Fig. 4. Effect of closed-loop control. (a) Measurement made without closed-loop feedback. The pressure steadily decreases along with the IR dc component. At approximately 160 s, the subject performed deep breathing resulting in a sudden pressure drop. Here, the IR level actually increases, suggesting that the applied pressure is now higher than MAP. This is also indicated by the diminishing IR pulse pressure. (b) Pulse morphology analysis during pressure changes with and without closed-loop feedback. Each curve represents an averaged pulse waveform at different heights from the heart level.

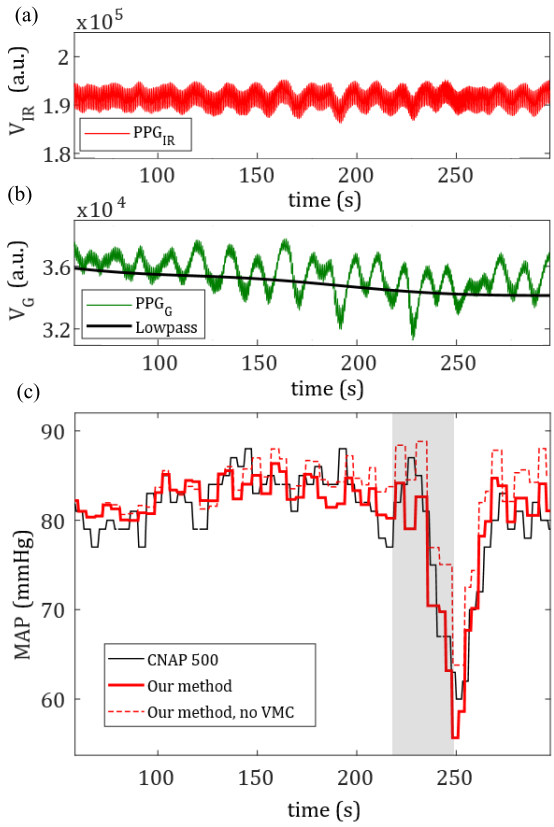

Fig. 5. First two plots show the behavior of (a) IR and (b) green PPG signals during closed-loop control. The IR dc component is held at a constant level. The green dc level shows a slight decrease during the measurement. (c) MAP recorded with the reference device and our method, with and without VMC. At approximately 220 s, the subject initiated fast breathing (indicated by the gray area), which is seen as a sudden drop in BP followed by a fast BP surge.

lower the pressure, lowering the IR dc component as well. In green PPG, the effect of deep breathing is less pronounced.

It is well known that the pulse waveform depends on the prevalent P_t. This effect is seen both in pressure and optical signals. To study the effect of contact pressure on pulse wave morphology, we used a power-adjustable desk to create a hydrostatic pressure change in the hand. We raised and lowered the desk 10 cm with the subject's hand placed on it and compared the corresponding waveforms to the initial waveform at zero P_t. The pulse is undistorted at zero P_t. The procedure was repeated with and without feedback. With the feedback loop on, the waveform remained very similar to the original, indicating that P_t had not changed. Correspondingly, with the feedback loop switched off, the level shift resulted in a significant change in the pulse morphology. When the arm was lowered from the heart level, P_t turned positive, resulting in a sharp and pointy pulse. When raised, P_t turned negative and the pulse had a more smooth and wide appearance. In both cases, the amplitude of the pulse decreased when the applied pressure diverged from MAP, but for comparison purposes, all pulses are normalized in Fig. 4(b).

B. Dynamic BP Changes

To experimentally validate the method, its ability to maintain zero P_t for continuous tracking of MAP was assessed by comparing simultaneous recordings with the reference device and our device. We analyzed the measurements by dividing each measurement into 10-s epochs and computed the mean value for each segment for both our and the reference device. Comparing data from both devices resulted in [(mean $\pm$ SD) mmHg] of (0.1 $\pm$ 4.4) mmHg for MAP. The data are displayed in correlation and Bland–Altman plots in Fig. 6(b) [31]. The measured MAP tracked the reference very closely during the BP-altering maneuvers. In the measurement shown in Fig. 5(a), the sudden drop in BP caused by fast breathing was as high as 20 mmHg, happening over 15 s. The PID controller was able to react to these relatively fast changes. In a real use case, the changes in BP would presumably rarely be faster than these, particularly for home use. In a hospital environment, the changes could be more dramatic. A sudden blood loss during hemorrhage could be simulated with a negative lower body negative pressure test to verify operation in extreme conditions [32].

C. Vasomotor Tone and Compensatory Postprocessing

It has been disclosed since the early days of VUT that vasomotor action, vasodilation, and vasoconstriction alter the

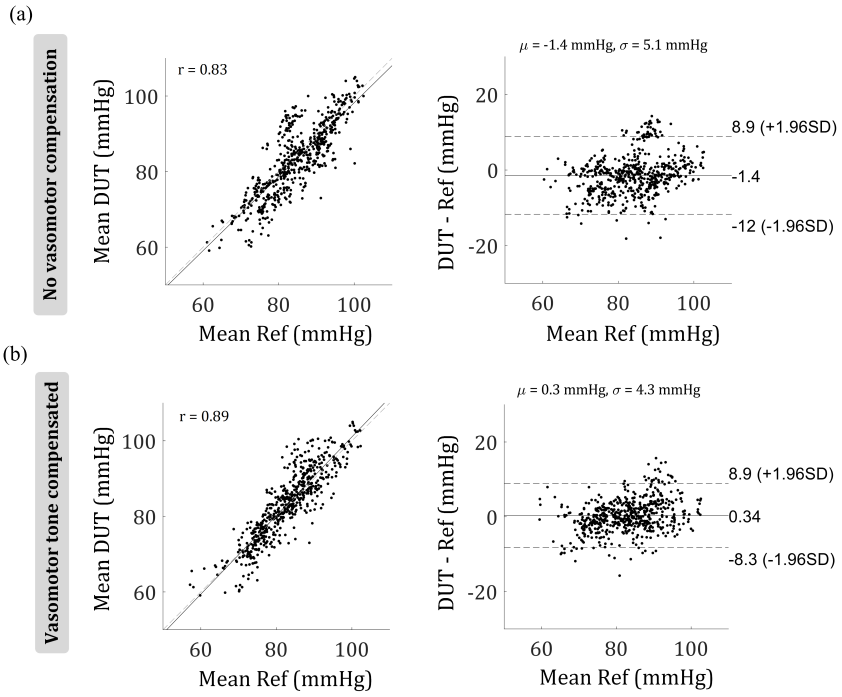

Fig. 6. Results. (a) Bland–Altman plots of the measurements with [(0.3 ± 4.3) mmHg] and (b) without [(-1.4 ± 5.1) mmHg] VMC.

pressure–volume curve of BP [20]. In practice, vasomotor action can lead to a divergence from the state of zero P_t consequently leading to a setpoint that is no longer valid.

To verify that the green dc-level is actually modulated by vasomotor tone, we assessed the changes in the green dc-level in comparison to the pulse shape alteration in clamped IR PPG. We tuned the PID controller to oscillate around the setpoint with a period time of approximately 7 s. The oscillation is used to induce periodic changes in P_t. This allows the P_t to vary around zero, periodically altering between positive and negative. Each pulse was integrated over to find the area under the curve (AUC) for each IR PPG cardiac cycle. Then, the AUC at the minimum P_t of each oscillation cycle ($\text{AUC}_{\text{IR}}@P_{t\_\text{min}}$), that is, at the highest point of oscillation, was recorded. When the setpoint starts to diverge from zero P_t due to vasomotor action, the IR PPG AUC at the highest point of each oscillation period increases or decreases depending on the direction of the change. If the $\text{AUC}_{\text{IR}}@P_{t\_\text{min}}$ decreases over multiple oscillation periods, we can assume that the current clamping pressure is too high and that P_t has decreased. On the other hand, if $\text{AUC}_{\text{IR}}@P_{t\_\text{min}}$ increases, we can assume that the clamping pressure is too low and that P_t has increased. Simultaneously, green PPG is recorded. We then compared the green dc component and the variation of $\text{AUC}_{\text{IR}}@P_{t\_\text{min}}$ during vasomotor action. Fig. 7 shows the behavior of the oscillating IR PPG and the principle of computing $\text{AUC}_{\text{IR}}@P_{t\_\text{min}}$ for each oscillation period. The $\text{AUC}_{\text{IR}}@P_{t\_\text{min}}$ changing over time is shown along with green PPG. This suggests that the green dc component actually tells if the system has diverged from zero P_t.

We then compared the Bland–Altman plot of the resulting signal in Fig. 6(b) to the one without vasomotor compensation in Fig. 6(a), in order to observe if there is an effect on accuracy when VMC is used. The term "accuracy" is defined in the context of BP measurement guidelines, which differs from the description used in the field of Instrumentation and Measurement [33], [34]. The plot with VMC showed better accuracy: (0.3 ± 4.3) mmHg compared to the original: (-1.4 ± 5.1) mmHg.

TABLE I
ABBREVIATED LIST OF EXISTING VUT DEVICES. *CNAP2GO IS IMPLEMENTED ON A CNAP 500 DEVICE, BUT CAN BE MINIATURIZED

Device	Technology	Vasomotor compensation	Cost	Source
Finapres	VUT	Physiocal	$$$	[21]
CNAP 500	VUT	VERIFI	$$$	[22], [29]
CNAP2GO	modified VUT	VERIFI	$$($)*	[24]
Our device	modified VUT	Green PPG	$	This work

CNAP2GO has an advantage over our dc-level method. Since it essentially relies on applying the VERIFI method without full VUT, it can reassess the setpoint without interruptions [22], [24]. Our method, on the other hand, does not necessarily require a high-quality pulse waveform and can withstand cold fingers based on this initial study. Moreover, our method does not require a cuff for applying pressure. However, similar to the cuff-based approach, our method still requires the external pressure to be held at zero P_t during the measurement. This causes venous pooling in the fingertip and noticeable discomfort to the user. In their paper, the researchers at CNSystems proposed that the pressure could be lowered to a more comfortable pressure and the data could be interpolated between the actual measurements [24].

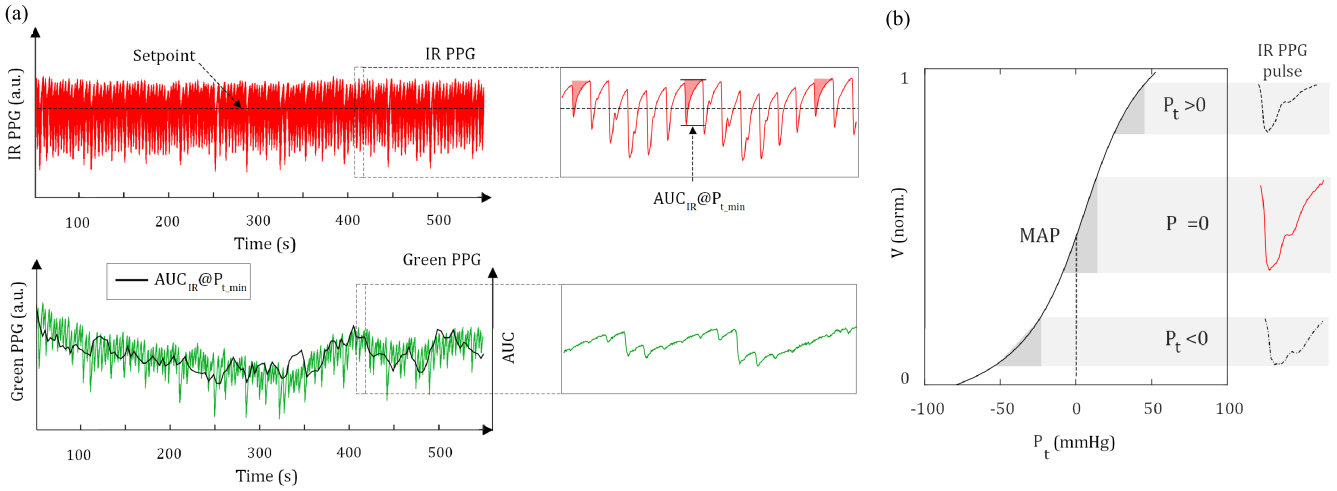

Fig. 7. (a) In the top, IR PPG is clamped to a setpoint, but allowed to oscillate around it. AUC for each IR pulse is assessed. This lets the green volume vary, reacting to vasomotor action. AUC for each IR pulse is assessed. For each oscillation cycle, we select the AUC at the minimum P_t level ($\text{AUC}_{\text{IR}}@P_{t\_\text{min}}$). These values are then plotted along with the green PPG level at the bottom. As can be seen in the closeup frame of the green PPG, the green PPG oscillates periodically similar to IR PPG, but presents a "wandering" baseline throughout the measurement. (b) Pressure–volume plot showing the change in IR PPG volume at different transmural pressures (P_t). The volume alteration is at its highest around MAP and decreases when P_t diverges from MAP.

IV. Discussion

The proposed method for controlling the fingertip blood volume on a beat-by-beat level by keeping the IR PPG dc component constant using a feedback loop that controls the pressure exerted on the finger shows promise in continuous BP monitoring. The proposed device is made with simple components and does not require volume clamping. Manufacturing tolerances and the gear set used would unlikely withstand such fast manipulation. Moreover, the motor would be running continuously, which increases the power consumption. In our method, the motor is driven for a minimum period between pulses.

1) Challenges: We also noticed some issues with the piston method. At the beginning of a measurement, especially after being unused for a while, the pressure sensor showed a decreasing trend at high pressures. This might be due to the deformation of the air cushion under stress. Partially, this might also be caused by pressure-induced vasodilation due to the finger being under high pressure. This makes the first few minutes of a measurement unreliable. Peňáz [20] also reported this problem in his experiments. When the contact pressure is correctly held at MAP, the blood flow through the arteries remains intact. However, some local venous pooling can occur and create pain. Additionally, the prolonged contact pressure could cause unwanted vasomotion during the measurement. This could be resolved by reducing the contact pressure by clamping to a lower volume setpoint as suggested by Fortin et al. [24]. There are still some improvements to be made in the next iteration of the device. The PID controller is very crude at the moment and would benefit from fine-tuning. Additionally, machine learning could be used to both tune the controller on the go and make adjustments to compensate for changes in vasomotor tone.

This study is meant to serve as a proof-of-concept of the technique. We recognize that the dataset used in this study is limited. However, the accuracy of the continuous BP measurement in any VUT method depends heavily on the accuracy of the oscillometric calibrations performed at certain intervals. This is usually done with a brachial cuff, but in our previous study, we have shown that it can be done robustly with the finger tonometry method [27], [35].

2) Future Directions: In the future, oscillometric MAP, along with systolic and diastolic values could be taken using the finger device. In our previous paper, we verified that BP can actually be measured accurately from the finger using tono-oscillometry [27]. The fingertip has actually been suggested to be the best location for oscillometric measurement [36]. However, since in this study, the additional electronics needed for obtaining the PPG signal were integrated into the piston, oscillometric BP could not be performed with high enough precision. This is nonetheless merely a matter of miniaturization and novel manufacturing engineering. This would eliminate the need for arm cuff devices and open up the possibility of tracking continuous BP from the finger only. In addition to the MAP, it is also possible to track systolic and diastolic BPs using brachial calibration as well. This could be achieved by monitoring either the pressure signal or IR PPG pulse pressure and scaling SBP and DBP accordingly, as described in [24]. The full pressure profile $P(t)$ can be calculated by superimposing the V_{IR} pulse to the mean BP signal (P_{MBP})

$$P(t) = P_{\text{MBP}}(t) + kV_{\text{IR}}(t)$$

and

$$k = \frac{\text{SBP}_{\text{init}} - \text{DBP}_{\text{init}}}{V_{\text{IR\_systole}} - V_{\text{IR\_diastole}}}$$

where SBP_{init} and DBP_{init} are the initial oscillometric values, and $V_{\text{IR\_systole}}$ and $V_{\text{IR\_diastole}}$ are the peak and foot values from the IR PPG pulse profile.

The proposed method offers a way to miniaturize continuous BP measurement technology. Since the full cardiac cycle does

not need to be clamped, there is no need for fast-switching pneumatics or a cuff. We have shown that much simpler pressure-applying techniques are sufficient for following BP trends. Comparison on the key features of similar devices is shown in Table I. The method is also compatible with continuous pulse oximetry, since the ac component of the PPG is allowed to pulsate freely. This feature is needed for computing peripheral oxygen saturation (SpO_2) [37]. The proposed device is already enclosed in a similar form factor as commercial pulse oximeter probes and can further be developed to work with a patient monitor. The method could alternatively be used to probe a different artery. VUT method has already been proven to work on radial and superficial temporal arteries [38], [39], [40]. Another direction of development could be health wearables. Fitting a rechargeable Li-ion battery and wireless communication, for example, Bluetooth, is possible. This would make nighttime monitoring much more convenient and unobtrusive. A key advantage of continuous monitoring is the ability to catch sudden changes in BP, such as in the presence of hypovolemic shock [41]. The low-frequency VUT technique is particularly useful for quickly noticing the change in BP, so an oscillometric measurement can be initiated.

V. Conclusion

We presented a technique and a device for continuous noninvasive BP monitoring using nonpulsatile, or dc, PPG components in a wearable form factor. Requiring less complex mechanics, the beat-wise level volume clamping resulted in similar MAP tracking accuracy than traditional VUT. The error introduced by vasomotor changes poses a significant challenge to the IR dc clamping method. We noticed that when the IR wavelength PPG dc volume was clamped, the green wavelength dc-level varied in response to vasomotor action. This is likely due to vasomotor activity, which is mostly regulated by arterioles—the vessel green PPG probes. Using these dc components, we can continuously measure arterial BP and assess arteriolar vasomotor tone.

References

[1] A. Siu, "Screening for high blood pressure in adults: U.S. Preventive services task force recommendation statement," *Ann. Internal Med.*, vol. 163, no. 10, pp. 778–786, 2015.

[2] P. Muntner et al., "Measurement of blood pressure in humans: A scientific statement from the American heart association," *Hypertension*, vol. 73, no. 5, pp. e35–e66, 2019.

[3] K. Kario et al., "Nighttime blood pressure measured by home blood pressure monitoring as an independent predictor of cardiovascular events in general practice: The J-HOP nocturnal blood pressure study," *Hypertension*, vol. 73, no. 6, pp. 1240–1248, Jun. 2019.

[4] T. Panula, J.-P. Sirkia, D. Wong, and M. Kaisti, "Advances in non-invasive blood pressure measurement techniques," *IEEE Rev. Biomed. Eng.*, vol. 16, pp. 424–438, 2023.

[5] J. Penaz, "Photoelectric measurement of blood pressure, volume and flow in the finger," in *Proc. Digest 10th Int. Conf. Med. Biol. Eng.*, 1973.

[6] D. Nair et al., "The use of ambulatory tonometric radial arterial wave capture to measure ambulatory blood pressure: The validation of a novel wrist-bound device in adults," *J. Hum. Hypertension*, vol. 22, no. 3, pp. 220–222, Mar. 2008.

[7] K. G. Belani, J. J. Buckley, and M. O. Poliac, "Accuracy of radial artery blood pressure determination with the Vasotrac™," *Can. J. Anesthesia*, vol. 46, no. 5, pp. 488–496, 1999.

[8] R. Mukkamala et al., "Toward ubiquitous blood pressure monitoring via pulse transit time: Theory and practice," *IEEE Trans. Biomed. Eng.*, vol. 62, no. 8, pp. 1879–1901, Aug. 2015.

[9] G. Zhang, M. Gao, D. Xu, N. B. Olivier, and R. Mukkamala, "Pulse arrival time is not an adequate surrogate for pulse transit time as a marker of blood pressure," *J. Appl. Physiol.*, vol. 111, no. 6, pp. 1681–1686, 2011.

[10] A. Esmaili, M. Kachuee, and M. Shabany, "Nonlinear cuffless blood pressure estimation of healthy subjects using pulse transit time and arrival time," *IEEE Trans. Instrum. Meas.*, vol. 66, no. 12, pp. 3299–3308, Dec. 2017.

[11] K. Song, K.-Y. Chung, and J.-H. Chang, "Cuffless deep learning-based blood pressure estimation for smart wristwatches," *IEEE Trans. Instrum. Meas.*, vol. 69, no. 7, pp. 4292–4302, Jul. 2020.

[12] A. Chakraborty, D. Goswami, J. Mukhopadhyay, and S. Chakrabarti, "Measurement of arterial blood pressure through single-site acquisition of photoplethysmograph signal," *IEEE Trans. Instrum. Meas.*, vol. 70, pp. 1–10, 2021.

[13] M. P. D. Pont and J. L. B. Marques, "Reflective photoplethysmography acquisition platform with monitoring modules and noninvasive blood pressure calculation," *IEEE Trans. Instrum. Meas.*, vol. 69, no. 8, pp. 5649–5657, Aug. 2020.

[14] P. M. Nabeel, S. Karthik, J. Joseph, and M. Sivaprakasam, "Arterial blood pressure estimation from local pulse wave velocity using dual-element photoplethysmograph probe," *IEEE Trans. Instrum. Meas.*, vol. 67, no. 6, pp. 1399–1408, Jun. 2018.

[15] T.-W. Wang, W.-X. Chen, H.-W. Chu, and S.-F. Lin, "Single-channel bioimpedance measurement for wearable continuous blood pressure monitoring," *IEEE Trans. Instrum. Meas.*, vol. 70, pp. 1–9, 2021.

[16] J. Nyvad, K. L. Christensen, N. H. Buus, and M. Reinhard, "The cuffless SOMNOtouch NIBP device shows poor agreement with a validated oscillometric device during 24-h ambulatory blood pressure monitoring," *J. Clin. Hypertension*, vol. 23, no. 1, pp. 61–70, Jan. 2021.

[17] T. Panula, J.-P. Sirkia, and M. Kaisti, "Miniaturization of a finger-worn blood pressure instrument," in *Proc. 43rd Annu. Int. Conf. IEEE Eng. Med. Biol. Soc. (EMBC)*, Nov. 2021, pp. 7441–7444.

[18] I. Jeong, S. Jun, D. Um, J. Oh, and H. Yoon, "Non-invasive estimation of systolic blood pressure and diastolic blood pressure using photoplethysmograph components," *Yonsei Med. J.*, vol. 51, pp. 345–353, May 2010.

[19] T. Panula, J.-P. Sirkiä, and M. Kaisti, "Control method for continuous non-invasive arterial pressure monitoring using the non-pulsatile component of the PPG signal," in *Proc. Comput. Cardiol. (CinC)*, vol. 48, Sep. 2021, pp. 1–4.

[20] J. Penaz, "Criteria for set point estimation in the volume clamp method of blood pressure measurement," *Physiolog. Res.*, vol. 41, no. 1, pp. 5–10, 1992.

[21] K. Wesseling, "Finger arterial pressure measurement with finapres," *Zeitschrift Kardiologie*, vol. 85, pp. 38–44, Jan. 1996.

[22] J. Fortin, C. Fellner, N. Mocnik, J. Grond, T. Brunner, and D. Flotzinger, "The importance of VERIFI ('vasomotoric elimination and reconstructed identification of the initial set-point') for the performance of the CNAP technology," in *Proc. EMBEC NBC*. Cham, Switzerland: Springer, 2017, pp. 663–666.

[23] M. Intaglietta, "Vasomotion and flowmotion: Physiological mechanisms and clinical evidence," *Vascular Med. Rev.*, vol. -1, no. 2, pp. 101–112, Sep. 1990.

[24] J. Fortin et al., "A novel art of continuous noninvasive blood pressure measurement," *Nature Commun.*, vol. 12, no. 1, pp. 1–14, Mar. 2021.

[25] M. Kuwabara, K. Harada, Y. Hishiki, and K. Kario, "Validation of two watch-type wearable blood pressure monitors according to the ANSI/AAMI/ISO81060-2:2013 guidelines: Omron HEM-6410T-ZM and HEM-6410T-ZL," *J. Clin. Hypertension*, vol. 21, no. 6, pp. 853–858, Jun. 2019.

[26] A. V. Moço, S. Stuijk, and G. de Haan, "New insights into the origin of remote PPG signals in visible light and infrared," *Sci. Rep.*, vol. 8, no. 1, pp. 1–15, May 2018.

[27] T. Panula, T. Koivisto, M. Pänkäälä, T. Niiranen, I. Kantola, and M. Kaisti, "An instrument for measuring blood pressure and assessing cardiovascular health from the fingertip," *Biosensors Bioelectron.*, vol. 167, Nov. 2020, Art. no. 112483.

[28] J. G. Ziegler and N. B. Nichols, "Optimum settings for automatic controllers," *J. Fluids Eng.*, vol. 64, no. 8, pp. 759–765, Nov. 1942.

[29] R. Hahn, H. Rinösl, M. Neuner, and S. C. Kettner, "Clinical validation of a continuous non-invasive haemodynamic monitor (CNAP™ 500) during general anaesthesia," *Brit. J. Anaesthesia*, vol. 108, no. 4, pp. 581–585, Apr. 2012.

[30] World Medical Association, "World medical association declaration of Helsinki: Ethical principles for medical research involving human subjects," *JAMA*, vol. 310, no. 20, pp. 2191–2194, Nov. 2013.

[31] J. M. Bland and D. G. Altman, "Statistical methods for assessing agreement between two methods of clinical measurement," *Lancet*, vol. 327, no. 8476, pp. 307–310, Feb. 1986.

[32] G. J. Crystal and M. R. Salem, "Lower body negative pressure: Historical perspective, research findings, and clinical applications," *J. Anesthesia Hist.*, vol. 1, no. 2, pp. 49–54, Apr. 2015.

[33] G. S. Stergiou et al., "Recommendations and practical guidance for performing and reporting validation studies according to the universal standard for the validation of blood pressure measuring devices by the association for the advancement of medical instrumentation/European society of hypertension/international organization for standardization (AAMI/ESH/ISO)," *J. Hypertension*, vol. 37, no. 3, pp. 459–466, 2019.

[34] S. Shirmohammadi, K. Barbe, D. Grimaldi, S. Rapuano, and S. Grassini, "Instrumentation and measurement in medical, biomedical, and healthcare systems," *IEEE Instrum. Meas. Mag.*, vol. 19, no. 5, pp. 6–12, Oct. 2016.

[35] T. Panula et al., "Development and clinical validation of a miniaturized finger probe for bedside hemodynamic monitoring," *medRxiv*, vol. 2022, pp. 1–12, Jan. 2022.

[36] J. Liu, C. G. Sodini, Y. Ou, B. Yan, Y.-T. Zhang, and N. Zhao, "Feasibility of fingertip oscillometric blood pressure measurement: Model-based analysis and experimental validation," *IEEE J. Biomed. Health Informat.*, vol. 24, no. 2, pp. 533–542, Feb. 2020.

[37] T. L. Rusch, R. Sankar, and J. E. Scharf, "Signal processing methods for pulse oximetry," *Comput. Biol. Med.*, vol. 26, no. 2, pp. 143–159, Mar. 1996.

[38] S. Tanaka and K. Yamakoshi, "Ambulatory instrument for monitoring indirect beat-to-beat blood pressure in superficial temporal artery using volume-compensation method," *Med. Biol. Eng. Comput.*, vol. 34, no. 6, pp. 441–447, Nov. 1996.

[39] S. Tanaka, M. Nogawa, T. Yamakoshi, and K. I. Yamakoshi, "Accuracy assessment of a noninvasive device for monitoring beat-by-beat blood pressure in the radial artery using the volume-compensation method," *IEEE Trans. Biomed. Eng.*, vol. 54, no. 10, pp. 1892–1895, Oct. 2007.

[40] M. Ogawa, M. Nogawa, and K.-I. Yamakoshi, "Non-invasive measurement of instantaneous blood pressure in dorsalis pedis artery based on the volume-compensation technique," in *Proc. 4th Int. Congr. Image Signal Process.*, vol. 1, 2011, pp. 211–215.

[41] D. M. Kelley, "Hypovolemic shock: An overview," *Crit. Care Nursing Quart.*, vol. 28, no. 1, pp. 2–19, 2005.

Tuukka Panula received the B.Sc. (Tech.) degree in computer and electronics engineering and the M.Sc. (Tech.) degree in health technology from the University of Turku, Turku, Finland, in 2018 and 2019, respectively, where he is currently pursuing the Ph.D. degree in health technology.

From 2022 to 2023, he was with the Hamlyn Centre for Robotic Surgery, Imperial College London, London, U.K., where he worked on biomedical instrumentation as a Visiting Ph.D. Researcher for six months. He is currently working on blood pressure and hemodynamic monitoring at the University of Turku.

Jukka-Pekka Sirkiä received the B.Sc. and M.Sc. degrees in industrial engineering and management from the Tampere University of Technology, Tampere, Finland, in 2012 and 2015, respectively, and the M.Sc. degree in software engineering from the University of Turku, Turku, Finland, in 2020, where he is currently pursuing the Ph.D. degree.

Matti Kaisti received the B.Sc. degree in electrical engineering from the Turku University of Applied Sciences, Turku, Finland, in 2008, and the M.Sc. and Ph.D. (Hons.) degrees in electrical engineering from the University of Turku, Turku, in 2012 and 2017, respectively.

In his Ph.D. work, he studied field-effect-based biological and chemical sensing. From 2018 to 2019, he worked as a Postdoctoral Researcher with the Department of Bioengineering, Imperial College London, London, U.K. Currently, he works as an Assistant Professor with the University of Turku. His research interests include biomedical instrumentation, biomedical signal processing, and AI in healthcare.